JOURNAL OF BACTERIOLOGY, Jan. 2006, p. 115–123 Vol. 188, No. 1
0021-9193/06/$08.00+0 doi:10.1128/JB.188.1.115–123.2006

Mutations in the Central Cavity and Periplasmic Domain Affect Efflux Activity of the Resistance-Nodulation-Division Pump EmhB from *Pseudomonas fluorescens* cLP6a

Elizabeth M. Hearn,[1,2] Murray R. Gray,[2] and Julia M. Foght[1]*

Department of Biological Sciences, University of Alberta, Edmonton, Alberta, Canada T6G 2E9,[1] and Department of Chemical and Materials Engineering, University of Alberta, Edmonton, Alberta, Canada T6G 2G6[2]

Received 27 September 2005/Accepted 30 September 2005

The EmhABC efflux system in *Pseudomonas fluorescens* cLP6a is homologous to the multidrug and solvent efflux systems belonging to the resistance-nodulation-division (RND) family and is responsible for polycyclic aromatic hydrocarbon transport, antibiotic resistance, and toluene efflux. To gain a better understanding of substrate transport in RND efflux pumps, the EmhB pump was subjected to mutational analysis. Mutagenesis of amino acids within the central cavity of the predicted three-dimensional structure of EmhB showed selective activity towards antibiotic substrates. An A384P/A385Y double mutant showed increased susceptibility toward rhodamine 6G compared to the wild type, and F386A and N99A single mutants showed increased susceptibility to dequalinium compared to the wild type. As well, the carboxylic acid side chain of D101, located in the central cavity region, was found to be essential for polycyclic aromatic hydrocarbon transport and resistance to all antibiotic substrates of EmhB. Phenylalanine residues located within the periplasmic pore domain were also targeted for mutagenesis, and the F325A and F281A mutations significantly impaired efflux activity for all EmhB substrates. One mutation (A206S) in the outer membrane protein docking domain increased antibiotic resistance and toluene tolerance, demonstrating the important role of this domain in transport activity. These data demonstrate the roles of the central cavity and periplasmic domains in the function of the RND efflux pump EmhB.

Efflux pumps belonging to the resistance-nodulation-division (RND) family are prevalent in gram-negative bacteria, where they contribute to multidrug and solvent resistance (21, 23). The best-studied RND efflux pumps are AcrB in *Escherichia coli* and MexB in *Pseudomonas aeruginosa*, both of which pump a wide variety of structurally diverse compounds, including tetracycline, chloramphenicol, fluoroquinolones, and β-lactam antibiotics (20). One of the central questions concerning RND efflux pumps, which recognize and expel a wide variety of structurally diverse hydrophobic compounds, is the mechanism by which these proteins achieve their broad substrate specificity.

RND efflux pumps are integral membrane proteins characterized by a large periplasmic domain that is believed to interact with a periplasmic membrane fusion protein and an outer membrane factor protein, forming a three-component efflux system that efficiently expels substrates directly to the extracellular medium (20). The recently determined structure of the *E. coli* pump AcrB suggested an additional role for the periplasmic domain in substrate recognition and translocation (19). For the trimeric AcrB functional unit, Murakami et al. (19) proposed that substrates enter the pump through vestibules which extend from the external surface of the periplasmic domain and lead into a central cavity located between the transmembrane and periplasmic domains. Each monomer contributes an α-helix to form a central pore connecting the central cavity to the upper, funnel-shaped region of the pump, where substrates are predicted to enter the outer membrane channel (19). Evidence for a substrate transport pathway through the central cavity has been provided by cocrystallization of AcrB with several drugs, which demonstrated that substrates bind in the central cavity (31), and by mutagenesis studies (18) that established the importance of the central pore in AcrB pump function. Two studies using chimeric constructs of the *E. coli* AcrB and AcrD efflux pumps (6) and of the *E. coli* AcrB and *P. aeruginosa* MexB efflux pumps (29) showed the importance of the periplasmic domains in determining substrate specificity. Moreover, several residues, including E89 and F608, in the periplasmic domain of the *P. aeruginosa* MexD efflux pump were shown to be involved in substrate recognition and transport (15). Middlemiss and Poole (16) found a number of mutations within the MexB periplasmic and transmembrane domains that altered substrate selectivity likely by affecting tertiary structure or protein-protein interactions within the efflux complex. Neither the avenue through which substrates enter the central cavity nor the mechanism for substrate selectivity, both of which may involve the vestibules, has been elucidated.

Recently, an RND efflux system designated EmhABC, responsible for the export of polycyclic aromatic hydrocarbons, was identified for *Pseudomonas fluorescens* cLP6a (9). Polycyclic aromatic hydrocarbons represent a new class of efflux pump substrates that are highly hydrophobic but are not toxic to bacterial cells. In addition to polycyclic aromatic hydrocarbons, the EmhABC efflux system was involved in antibiotic

* Corresponding author. Mailing address: Department of Biological Sciences, CW405 Biological Sciences Center, University of Alberta, Edmonton, Alberta, Canada T6G 2E9. Phone: (780) 492-3279. Fax: (780) 492-9234. E-mail: julia.foght@ualberta.ca.

resistance of *P. fluorescens* cLP6a to chloramphenicol and nalidixic acid (9).

In the present study, the substrate specificity of the EmhB pump was broadened to include rhodamine 6G, dequalinium, ciprofloxacin, and toluene, and the basis for the substrate specificity of the EmhABC efflux system was investigated by using mutational analysis of the EmhB pump protein. Amino acids in both the periplasmic pore domain and the outer membrane protein docking domain were found to influence efflux activity and substrate specificity of the EmhB pump.

MATERIALS AND METHODS

Bacterial strains, plasmids, and growth conditions. *P. fluorescens* cLP6a-1, which has a disrupted copy of the chromosomal *emhB* gene, was constructed by insertional mutagenesis as described previously (9). Liquid cultures of the *P. fluorescens* cLP6a-1 strains were grown from a 0.5% (vol/vol) inoculum of an overnight, 10-ml seed culture in 200 ml tryptic soy broth (Difco Laboratories, Detroit, Mich.) at 28°C with shaking (200 rpm). *E. coli* DH5α (26) and XL10-Gold (Stratagene, La Jolla, California) strains were used for DNA manipulation and were cultured in Luria-Bertani (LB) medium at 37°C. Plasmid pCR2.1 (Invitrogen Canada, Burlington, Ontario, Canada) was used as a cloning vector. Plasmid pBH5, a derivative of the broad-host-range vector pUCP26 (30) that contains the *emhABC* genes, was constructed previously (9). *P. fluorescens* cLP6a-1 strains carrying plasmids were cultured in the presence of tetracycline (10 μg ml^{-1}).

DNA techniques. Molecular techniques, including plasmid DNA isolation, restriction digestion, and ligation reactions, were performed according to the suppliers' directions (QIAGEN, Mississauga, Ontario, Canada, and Roche Diagnostics, Laval, Quebec, Canada). Nucleotide sequencing reactions were performed using a BigDye Terminator cycle sequencing kit (Applied Biosystems, Inc., Foster City, California), and the results were analyzed with a model 373A automated DNA sequencer (Applied Biosystems, Inc.) by the Molecular Biology Services Unit (University of Alberta, Edmonton, Alberta, Canada). Nucleotide sequence data were analyzed with the GeneTool 1.0 software package (BioTools, Inc., Edmonton, Alberta, Canada).

Construction of histidine-tagged EmhB. An oligonucleotide encoding a six-histidine tag was introduced in frame at the 3′ end of the *emhB* gene by using the overlap extension PCR method (10). The primers used were EMH1, 5′-GGACTGAACGACGAGCCGCAATAT-3′; EMH2, 5′-ATTAGTGATGGTGATGGTGGTGGCCAGCCTCTTTAGAAGGTTCAATAGC-3′; EMH3, 5′-GGCCACCACCATCACCATCACTAATGAGCAAGTCGCTACTCTCCATCG-3′; and EMH4, 5′-CAGGAAACAGCTATGACCATGATTACGA-3′ (underlined nucleotides correspond to the codons for the histidine tag). The resulting PCR product was digested with EcoRI and ligated into EcoRI-digested pBH5 to replace the corresponding region in the plasmid. The new plasmid carrying the histidine-tagged *emhB* gene was designated pBH5-EmhB_{His} and was transformed into *P. fluorescens* cLP6a-1 by electroporation. Nucleotide sequencing of the 4.6-kb EcoRI region in plasmid pBH5-EmhB_{His} confirmed the in-frame addition of six histidine codons at the 3′ end of the *emhB* gene and the absence of PCR-introduced errors.

Construction of site-directed mutations in EmhB_{His}. Mutations in the *emhB_{His}* gene were introduced by PCR using a QuikChange II XL site-directed mutagenesis kit (Stratagene). To facilitate the QuikChange reaction, a 3.8-kb fragment of the *emhA* and *emhB* genes spanning the unique BsiWI and XhoI restriction sites was amplified from pBH5-EmhB_{His} by PCR with primers BHN20, 5′-GGTCGACGAACAGGCGGTGAG-3′, and BHN38, 5′-CCCAGAAGATCGCCAGAACC-3′, corresponding to positions 1287 to 1307 and 5118 to 5137, respectively, in the nucleotide sequence (GenBank accession number AY349612). The 3.8-kb PCR product was cloned into pCR2.1 by using a TOPO TA cloning kit (Invitrogen Canada), and the resulting plasmid, pBH10, was used as the template in the QuikChange reaction. The QuikChange reaction (50 μl) contained 20 or 100 ng of pBH10 template DNA, 1× QuikChange buffer, 3 μl Quiksolution, 1 μl deoxynucleoside triphosphate mix, 1 μl *Pfu*Ultra, and forward and reverse mutagenic primers at a concentration of 12 μM each. The PCR cycles consisted of an initial denaturation at 95°C for 1 min, 18 cycles of 95°C for 50 s, 60°C for 50 s, and 68°C for 8 min, and a final extension at 68°C for 7 min. Following the PCR, the template plasmids were digested with DpnI, and the mutated pBH10 plasmids were transformed into *E. coli* XL10-Gold or DH5α. To replace the wild-type *emhB_{His}* gene on plasmid pBH5-EmhB_{His}, the 3-kb BsiWI-XhoI fragments from the mutated pBH10 plasmids were ligated into BsiWI-XhoI-digested pBH5-EmhB_{His}. The resulting plasmids, carrying the mutated *emhB_{His}* genes, were transformed into *P. fluorescens* cLP6a-1 by electroporation. Nucleotide sequencing was performed to confirm the mutations.

SDS-PAGE and Western immunoblotting analysis. To confirm expression of the mutated EmhB_{His} proteins in *P. fluorescens* cLP6a-1, sodium dodecyl sulfate-polyacrylamide gel electrophoresis (SDS-PAGE) and Western immunoblotting were performed on whole-cell extracts. Cells were harvested, resuspended in SDS-PAGE sample buffer (0.225 M Tris-HCl [pH 6.8], 5% [wt/vol] SDS, 0.05% [wt/vol] bromophenol blue, 0.25 M dithiothreitol, and 50% [vol/vol] glycerol), and heated for 10 min at 95°C. Samples containing 10 μg protein were separated by SDS-PAGE using a 6% resolving gel and transferred to Hybond-P membranes (Amersham Biosciences) by electroblotting using a Mini-Protean 3 electrophoretic transfer cell (Bio-Rad Laboratories). Immunoblotting with a Penta-His horseradish peroxidase conjugate (QIAGEN) was performed according to the manufacturer's protocols, and detection was carried out with a chemiluminescence kit (Amersham Biosciences).

Polycyclic aromatic hydrocarbon transport assays. The levels of accumulation of radiolabeled hydrocarbon substrate in the various strains were measured by using the rapid centrifugation method as described by Bugg et al. (4) and used previously (9). The radiolabeled hydrocarbon substrate, either [9-^{14}C]phenanthrene (96.5% radiochemical purity, 19.3 mCi $mmol^{-1}$; Amersham, Arlington Heights, Illinois) or [side ring U-^{14}C]anthracene (98% pure, 45 mCi $mmol^{-1}$; Amersham), was mixed with unlabeled compound and added to cell suspensions at final concentrations of 6.4 μM for phenanthrene and 0.26 μM for anthracene, which corresponded to 90% of the aqueous solubility limit for each compound. Steady-state measurements of the amount of substrate present in the cells were taken in duplicate following addition of the substrate to the cell suspension (approximately 10 min) and following addition of the energy inhibitor, 30 mM sodium azide (approximately 10 min after addition of azide).

Antibiotic sensitivity assays. The MICs of chloramphenicol, nalidixic acid, rhodamine 6G, dequalinium chloride, ciprofloxacin, and streptomycin were determined for the *P. fluorescens* strains in tryptic soy broth by the microtiter broth dilution method (11). The optical density at 600 nm of the microtiter cultures was measured using a SpectraMax Plus^{384} microplate reader (Molecular Devices Corporation, Sunnyvale, California). The MIC was defined as the lowest concentration of antibiotic that inhibited growth by more than 50% compared with a control grown in the absence of antibiotic.

Determination of toluene tolerance. Growth on solid media in the presence of vapor phase toluene was used to assess toluene tolerance resulting from the presence or absence of the EmhABC efflux system. Toluene (about 5 ml) was placed in a glass petri dish in the bottom of a sealed container and incubated at 28°C overnight to allow the air in the container to become saturated with toluene. Since *P. fluorescens* does not grow on toluene, the test strains were plated on LB agar containing the appropriate antibiotics, placed inside the toluene-saturated container, and incubated at 28°C. As a control, duplicate plates were incubated in the absence of toluene. After 4 days, the plates were removed from the toluene container and further incubated for 4 days in the absence of toluene to assess the viability of the cultures.

Protein modeling. The three-dimensional structure of EmhB was predicted by homology modeling with AcrB (19) (Protein Data Bank [PDB] entry 1IWG [http://www.pdb.org]) by using the SWISS-MODEL protein structure homology-modeling server (8). Structural representations of the EmhB model were generated by using the DS ViewerPro version 6.0 software (Accelrys, San Diego, Calif.).

RESULTS

Homology modeling of the EmhB efflux pump. Because EmhB and the *E. coli* RND efflux pump AcrB share 67% protein sequence identity and 78% protein sequence similarity, homology modeling of the EmhB protein sequence onto the AcrB crystal structure provided a reliable estimation of the EmhB structure. Like AcrB, the predicted three-dimensional structure of EmhB (Fig. 1) revealed three distinct domains: a transmembrane domain, which has been implicated in proton translocation (3, 7); a periplasmic pore domain, which contains a channel leading from a central cavity above the transmembrane domain; and an outer membrane protein docking domain, which is believed to associate with the outer membrane channel.

EmhB and EmhB_{His} pump polycyclic aromatic hydrocarbons, antibiotics, and toluene. Previously, it was shown that the EmhABC system was responsible for polycyclic aromatic hy-

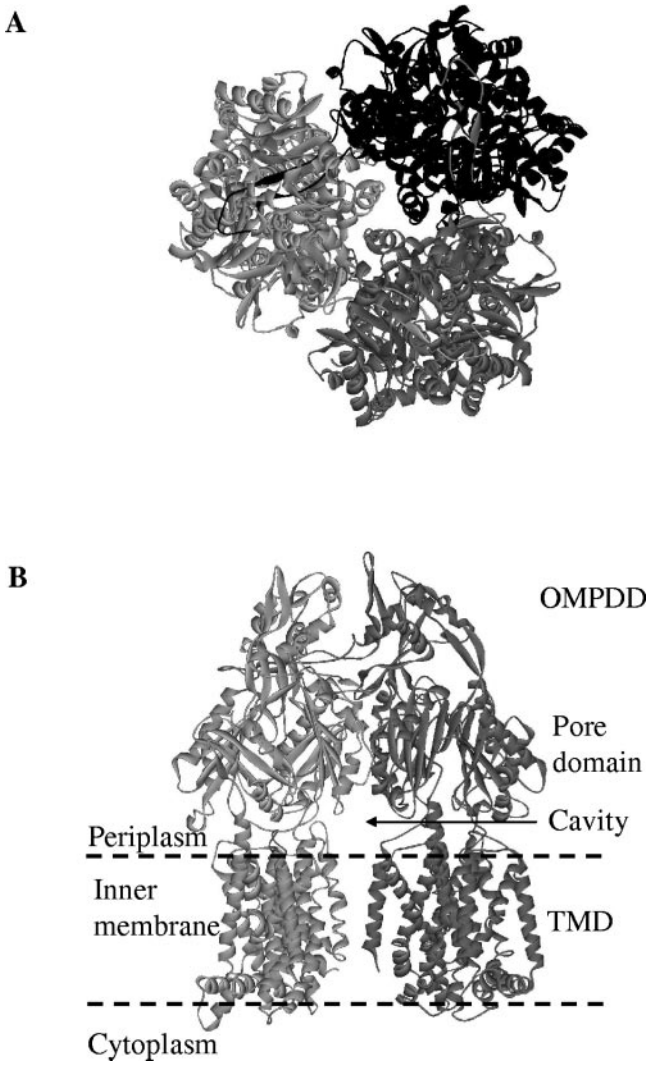

FIG. 1. Predicted structure of the EmhB efflux pump, modeled using the known crystal structure of the *E. coli* pump AcrB (PDB entry 1IWG [19]). (A) The view of the predicted EmhB trimer from above the plane of the inner membrane shows the presence of a pore extending through the pump. (B) The transmembrane domain (TMD), pore domain, and outer membrane protein docking domain (OMPDD) are indicated on the side view of the EmhB trimer, with the rear monomer removed to facilitate viewing. A central cavity is present at the center of the pump above the transmembrane domain. This figure and Fig. 3, 4, and 5 were drawn using the DS ViewerPro version 6.0 software (Accelrys).

drocarbon transport and antibiotic resistance to chloramphenicol and nalidixic acid in *P. fluorescens* cLP6a (9). To confirm that the histidine-tagged $EmhB_{His}$ pump was fully functional, the activity of *P. fluorescens* cLP6a-1 expressing $EmhB_{His}$ was compared to that of *P. fluorescens* cLP6a-1 expressing the wild-type EmhB pump and to that of a negative control, *P. fluorescens* cLP6a-1 pUCP26, which does not express EmhB (Table 1). In Table 1, the ability to transport the polycyclic aromatic hydrocarbons phenanthrene and anthracene is reported as the ratio of the amount of hydrocarbon accumulated in the cells prior to (uninhibited) and after (inhibited) addition of the energy inhibitor azide. Previous data indicated that cells possessing an active efflux system for polycyclic aromatic hydrocarbons accumulated approximately twofold less hydrocarbon in the absence of azide than in the presence of the inhibitor (9) and, thus, have a ratio of uninhibited/inhibited hydrocarbon transport of about 0.5. In contrast, cells that do not have an active efflux system for hydrocarbons showed no change in the cellular accumulation of hydrocarbon in the absence or presence of azide (9) and, thus, have a ratio of uninhibited/inhibited hydrocarbon transport of 1. As expected, the strains expressing both EmhB and $EmhB_{His}$ showed active efflux of phenanthrene and anthracene, while the negative control did not (Table 1).

The abilities of EmhB and $EmhB_{His}$ to pump antibiotics were also compared. As shown previously (9), chloramphenicol and nalidixic acid are substrates of the EmhB efflux pump, as *P. fluorescens* cLP6a-1 expressing the wild-type EmhB protein showed higher levels of resistance to these antibiotics than the negative-control strain (Table 1). The MICs for rhodamine 6G, dequalinium, and ciprofloxacin were significantly greater for the wild type and complemented strains expressing EmhB than those for the negative control and disrupted mutant (Table 1), indicating that these antibiotics are also substrates of the efflux pump. Although the MICs for *P. fluorescens* cLP6a-1 expressing $EmhB_{His}$ were lower for chloramphenicol and nalidixic acid than those for complemented EmhB, the MICs were still significantly higher than those for the negative control and disrupted mutant. The MICs for rhodamine 6G, dequalinium, and ciprofloxacin were comparable for the strains expressing the $EmhB_{His}$ and EmhB pumps. Streptomycin was not a substrate of either the EmhB efflux pump, as demonstrated previously (9), or the $EmhB_{His}$ pump (Table 1). Thus, the presence of the histidine tag slightly decreased the efficiency of the efflux system compared to that of the wild type but did not alter the specificity of the efflux pump for the antibiotics tested.

In a previous study, *P. fluorescens* cLP6a was unable to tolerate high concentrations of toluene in liquid medium and it was concluded on this basis that the EmhABC efflux system did not pump toluene (9). In the present study, toluene tolerance was assessed by monitoring growth on solid media (LB agar) in the presence of vapor phase toluene. *P. fluorescens* cLP6a was unable to grow on LB agar in the presence of vapor phase toluene but remained viable, as growth was observed upon removal from the toluene environment and further incubation (Table 1). In contrast, the *emhB* disruption mutant *P. fluorescens* cLP6a-1 was unable to recover upon removal of the toluene vapors (Table 1). Although the presence of the EmhABC efflux system in *P. fluorescens* cLP6a does not confer toluene tolerance, it does play a role in the ability of *P. fluorescens* cLP6a to remain viable in the presence of vapor phase toluene. These data suggest that, like the SrpABC efflux system in *Pseudomonas putida* S12 (13) and the Ttg efflux system in *P. putida* DOT-T1E (25), toluene is a substrate of the EmhB pump. Surprisingly, *P. fluorescens* cLP6a-1 complemented with the EmhABC efflux system on plasmid pBH5 was able to grow on LB agar in the presence of vapor phase toluene (Table 1). It is possible that the efflux genes were expressed at a higher level from the multicopy plasmid than from the chromosome in the wild-type *P. fluorescens* cLP6a, and increased expression of the pump may have led to an enhanced ability to tolerate toluene in the complemented mutant. The *P. fluorescens* cLP6a-1 strain ex-

TABLE 1. Effects of mutations of the efflux protein EmhB on polycyclic aromatic hydrocarbon transport, antibiotic sensitivity, and toluene tolerance in *P. fluorescens* cLP6a-1

Strain or mutation[a]	Hydrocarbon transport (ratio of uninhibited/inhibited)[b]		Antibiotic sensitivity (MIC, μg ml^{-1})[c]						Toluene tolerance[d]	
	Phenanthrene	Anthracene	Chl	Nal	R6G	Dq	Cip	Str	Growth	Recovery
Strains										
cLP6a (wild type)	0.40 ± 0.20 (3)	0.33 ± 0.11 (3)	16	16	>128	4	0.031	8	−	+
cLP6a-1 (disrupted EmhB)	0.86 ± 0.09 (3)	0.75 ± 0.16 (3)	2	1	4	0.5	0.004	4	−	−
cLP6a-1 (pUCP26) (negative control)	1.06 ± 0.05 (9)	0.90 ± 0.11 (6)	0.5	1	8	1	0.004	1	−	−
$EmhB_{His}$	0.53 ± 0.07 (9)	0.48 ± 0.13 (6)	8	32	128	8	0.031	2	−	+
EmhB (complemented control)	0.56 ± 0.08 (3)	0.56 ± 0.07 (3)	32	128	>128	8	0.063	1	+	+
Central cavity mutations										
A384P/A385Y	0.61	0.67	4	16	32	2	0.016	2	−	+
F386A	0.52	0.50	8	32	>128	2	0.016	1	−	+
F458A	0.55	0.56	8	16	64	4	0.016	1	−	+
F459A	0.60	0.56	8	16	64	4	0.016	1	−	+
N99A	0.53	0.49	4	32	64	2	0.031	1	−	+
D101A	0.84	0.96	1	16	16	1	0.016	2	−	+
D101N	0.80	0.70	2	16	32	2	0.016	1	−	+
D101E	0.50	0.47	8	32	>128	4	0.016	4	−	+
Pore domain mutations										
F316A	0.52	0.50	16	32	32	4	0.016	1	−	+
F317A	0.46	0.48	4	16	64	4	0.016	2	−	+
F682A	0.46	0.44	8	32	>128	4	0.016	2	−	+
F281A	0.90	0.83	<0.5	8	32	2	0.008	4	−	−
F325A	0.88	0.76	2	8	16	2	0.008	2	−	−
N282A	0.71	0.74	1	8	32	2	0.016	4	−	+
Outer membrane protein docking domain mutation										
A206S	0.48	0.53	32	128	>128	16	0.125	2	+	+

[a] Except for the wild type, all EmhB pumps were expressed in the efflux-deficient mutant *P. fluorescens* cLP6a-1 on the broad-host-range plasmid pUCP26. The negative control was *P. fluorescens* cLP6a-1 carrying the vector (pUCP26) only.

[b] For the strains expressing the $EmhB_{His}$ (pBH5-$EmhB_{His}$) and EmhB (pBH5) proteins and for the negative-control strain (pUCP26), the averages ± standard deviations are given, and the numbers in parentheses indicate the number of independent experiments performed. All other transport data are the averages of duplicate samples taken from single experiments.

[c] MICs were determined using the microtiter broth dilution method (11). Two independent experiments were done, and representative data are shown. Abbreviations: Chl, chloramphenicol; Nal, nalidixic acid; R6G, rhodamine 6G; Dq, dequalinium chloride; Cip, ciprofloxacin; and Str, streptomycin.

[d] Toluene tolerance was assessed by monitoring growth on LB agar plates in the presence of vapor phase toluene. Growth in the presence of toluene was scored as + (positive for growth) or − (negative for growth). The ability of the strains to recover from toluene exposure was scored as + (growth upon removal of toluene) or − (no growth upon removal of toluene). Two independent experiments were done.

pressing $EmhB_{His}$, however, was unable to grow in the presence of toluene vapors, although it did recover upon removal of the toluene (Table 1), similarly to *P. fluorescens* cLP6a.

Construction of site-directed mutants in $EmhB_{His}$. Mutations were introduced in $EmhB_{His}$ to confirm expression of the mutant pumps and to compare the activities of the mutant pumps for polycyclic aromatic hydrocarbons, antibiotics, and toluene relative to $EmhB_{His}$. Ten mutations (A384P, A385Y, A384P/A385Y, F386A, F458A, F459A, N99A, D101A, D101N, and D101E) were constructed in the central cavity region and seven mutations (Y157A, F316A, F317A, F682A, F281A, N282A, and F325A) were constructed in the pore domain of the histidine-tagged $EmhB_{His}$ protein by using site-directed mutagenesis. One mutation (A206S) in the outer membrane protein docking domain of $EmhB_{His}$ was obtained by a PCR-introduced error. The mutations were constructed in a histidine-tagged $EmhB_{His}$ to facilitate analysis of their expression in the *emhB* disruption mutant *P. fluorescens* cLP6a-1. Western immunoblotting (Fig. 2) showed that one mutant protein, A385Y in the central cavity, was not expressed and two mutant proteins, A384P and Y157A, were expressed poorly in *P. fluorescens* cLP6a-1. All other mutant proteins were expressed at levels comparable to $EmhB_{His}$.

The central cavity provides a flexible binding pocket for substrates during transport. The three-dimensional structure of the *E. coli* AcrB efflux pump identified a cavity between the transmembrane domain and the periplasmic domain (19), and cocrystallization of AcrB with bound drugs demonstrated the importance of this region in substrate binding (31). The EmhB central cavity (Fig. 3) is bound on the bottom (closest to the inner membrane) by residues A384, A385, F386, F458, and F459 and on the top (farthest from the inner membrane) by residues N99 and D101 from the N-terminal end of the pore-forming helices. A protein sequence alignment of EmhB with the homologous multidrug and solvent efflux pumps ArpB and SrpB from *P. putida* S12, TtgB, TtgE, and TtgH from *P. putida* DOT-T1E, MexB from *P. aeruginosa*, and AcrB from *E. coli* revealed that F386, F458, F459, and D101 are highly conserved (Table 2). Mutations in $EmhB_{His}$ were designed to target these residues lining the central cavity.

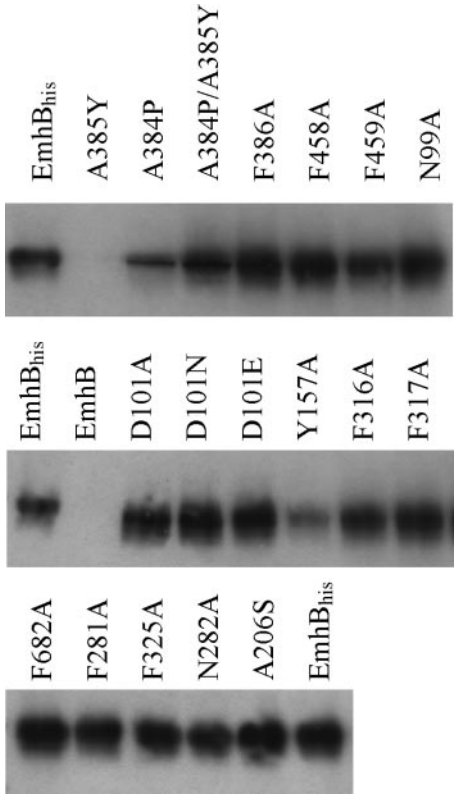

FIG. 2. Expression of mutant $EmhB_{His}$ proteins in *P. fluorescens* cLP6a-1 relative to $EmhB_{His}$ expression. Cell extracts (10 μg total protein) from *P. fluorescens* cLP6a-1 carrying the mutant $EmhB_{His}$ proteins were separated by SDS-PAGE and subjected to immunoblotting with an antibody against the histidine tag. The proteins are indicated above the lanes.

P. fluorescens cLP6a-1 expressing the A384P/A385Y double mutation in $EmhB_{His}$ showed significant (fourfold) decreases in antibiotic resistance to rhodamine 6G and dequalinium compared to resistance levels for the complemented control and $EmhB_{His}$ strains (Table 1). Dequalinium resistance was also reduced in the F386A and N99A mutant pumps (Table 1). The F458A and F459A mutations yielded only twofold decreases in resistance to many of the antibiotic substrates of EmhB. The A384P/A385Y, F386A, F458A, F459A, and N99A mutations in the central cavity did not affect efflux activity for polycyclic aromatic hydrocarbons and toluene. However, mutation of the highly conserved D101 residue to either alanine or asparagine greatly reduced the ability of the efflux pump to transport the polycyclic aromatic hydrocarbons phenanthrene and anthracene. The D101A and D101N mutations also resulted in significant (more than fourfold) decreases in antibiotic resistance for chloramphenicol, rhodamine 6G, and dequalinium and twofold decreases in nalidixic acid and ciprofloxacin resistance. Conservation of the carboxyl group on the amino acid side chain by mutation to glutamate (D101E) restored function of the efflux pump. These data support the involvement of the central cavity region for the activity of RND efflux pumps.

Amino acids in the pore domain influence efflux activity. Figure 4 shows the predicted model for the periplasmic pore domain of EmhB, with the three main regions identified by

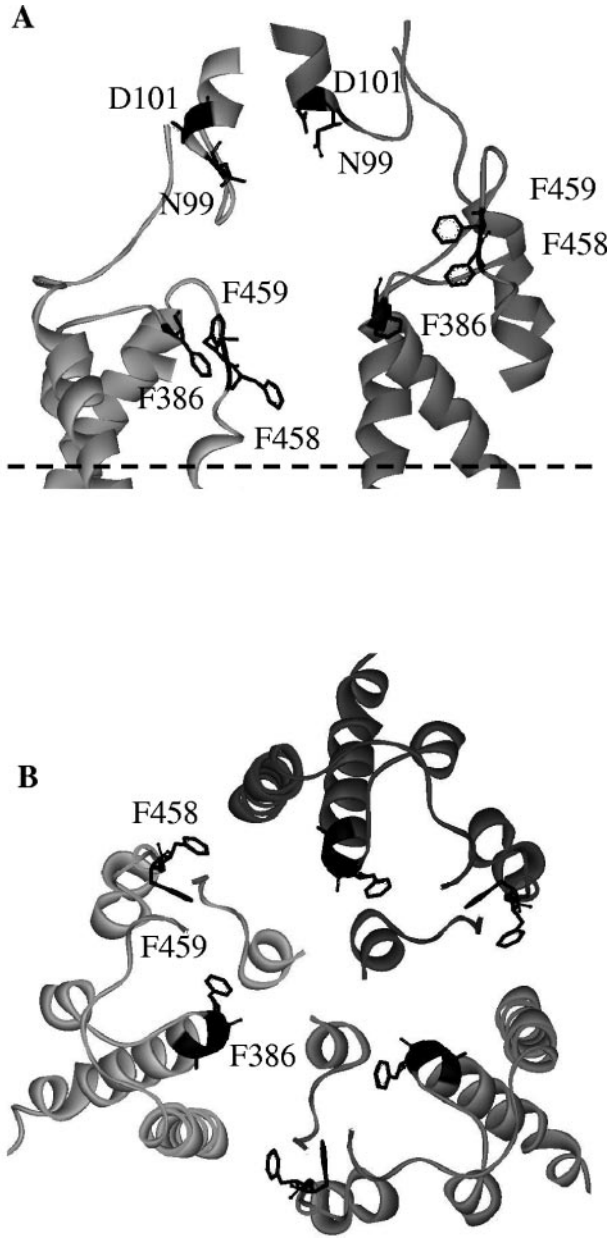

FIG. 3. Predicted model of the central cavity in EmhB. (A) The central cavity is viewed from the side parallel to the membrane, and the front monomer of EmhB is removed for ease of viewing. The N99, D101, F386, F458, and F459 residues lining the cavity are indicated. The A384 and A385 residues are not shown for ease of viewing. (B) A top view of the central cavity perpendicular to the plane of the membrane shows a ring formed by the residues F386, F458, and F459.

Murakami et al. (19): a central pore bounded by an α-helix from each subunit, a cleft in the center of each subunit, and three channels, or vestibules, located between the subunits. The presence of the three vestibules leading into the central cavity suggested that these are involved in substrate recognition and transport (19). Other studies have implicated the periplasmic domain in substrate recognition and specificity, as well as in the interaction between the efflux pump and the membrane fusion protein (5, 6, 15, 29). Because EmhB pumps

TABLE 2. Conservation of amino acid residues mutated in EmhB in RND multidrug and solvent efflux pumps[a]

Efflux pump[c]	Mutated residue in EmhB[b]														
	Central cavity							Pore domain							Outer membrane protein docking domain
	A384	A385	F386	F458	F459	N99	D101	Y157	F316	F317	F682	F281	F325	N282	A206
ArpB	**A**	**A**	A	**F**	**F**	**N**	**D**	**Y**	**F**	**F**	**F**	**F**	**F**	**N**	**A**
TtgB	**A**	**A**	A	**F**	**F**	**N**	**D**	**Y**	**F**	**F**	**F**	**F**	**F**	**N**	**A**
MexB	**A**	**A**	**F**	**F**	**F**	D	**D**	**Y**	**F**	M	**F**	**F**	Y	**N**	**A**
SrpB	P	Y	**F**	**F**	**F**	D	**D**	L	Y	L	Y	Y	Y	K	**A**
TtgH	P	Y	**F**	**F**	**F**	D	**D**	L	Y	L	Y	Y	Y	K	**A**
TtgE	P	Y	**F**	**F**	**F**	**N**	**D**	L	Y	L	Y	Y	Y	R	**A**
AcrB	**A**	**A**	**F**	**F**	**F**	D	**D**	**Y**	**F**	**F**	E	**F**	Y	**N**	**A**
MexD	Y	L	L	**F**	M	D	**D**	**Y**	**F**	**F**	R	L	V	**N**	**A**
MexY	L	G	L	**F**	**F**	**N**	**D**	I	Y	**F**	R	V	I	**N**	**A**

[a] Protein sequences were aligned by using ClustalX (28).
[b] Residues that are conserved in EmhB are indicated in boldface type.
[c] ArpB (GenBank accession number AAF73832 [12]) and SrpB (AAD12176 [13]) from *P. putida* S12; TtgB (AAC38671 [24]), TtgH (AAK69564 [25]), and TtgE (CAB72259 [17]) from *P. putida* DOT-T1E; MexB (NP_249117 [14]), MexD (NP_253288 [22]), and MexY (NP_250708 [1]) from *P. aeruginosa*; and AcrB (NP_414995 [19]) from *E. coli*.

polycyclic aromatic hydrocarbons, it was hypothesized that amino acids with aromatic side chains may be involved in hydrocarbon recognition and binding. Consequently, phenylalanines located within the pore domain were selected for mutagenesis in $EmhB_{His}$.

Two of the phenylalanines (F316 and F317) were located in the vestibule region of EmhB (Fig. 4). The F316A mutant $EmhB_{His}$ pump showed significant (fourfold) decreases in resistance to rhodamine 6G and ciprofloxacin and small (twofold) decreases in resistance to dequalinium compared to levels for the normal $EmhB_{His}$ (Table 1). The F317A mutant pump showed small (twofold) decreases in antibiotic resistance for all antibiotic substrates (Table 1). Neither the F316A nor the F317A mutation affected polycyclic aromatic hydrocarbon transport or toluene tolerance. Because F316 and F317 are located at the interface between EmhB monomers (Fig. 4), mutation of these residues likely disrupted interactions between the pump subunits, thereby reducing efflux activity for a number of substrates.

Among the phenylalanines selected for mutation in the periplasmic pore domain outside the vestibule region, one phenylalanine mutation (F682A) did not affect the transport of polycyclic aromatic hydrocarbons, hydrophobic antibiotics, or toluene (Table 1). However, the F281A mutation in $EmhB_{His}$ disrupted efflux activity not only for phenanthrene and anthracene but also for toluene and all of the antibiotic substrates tested (Table 1). Mutation of the neighboring F325 residue also inhibited $EmhB_{His}$ activity for all substrates, and mutation of the neighboring N282 residue partially inhibited polycyclic aromatic hydrocarbon transport and decreased resistance to antibiotics but not toluene (Table 1). The latter conclusion was based on the Grubbs test, which showed that the ratio of uninhibited to inhibited hydrocarbon transport was a statistical outlier from both the positive and the negative controls. The reduction of efflux activity for the $EmhB_{His}$ pumps with the F281A, F325A, and N282A mutations suggests that these residues may be involved in interactions with the membrane fusion protein or that these mutations altered the tertiary structure of the efflux pump, thereby compromising activity.

A mutation in the outer membrane protein docking domain enhances efflux activity. One EmhB mutant protein displayed increased levels of antibiotic resistance as well as the ability to grow in the presence of toluene (Table 1). The increased efficiency of the A206S mutant pump enhanced the growth of *P. fluorescens* cLP6a-1 in the presence of toluene and antibiotics, but the transport of polycyclic aromatic hydrocarbons appeared to be unaffected (Table 1). Small decreases in the steady-state levels of hydrocarbon may be undetectable due to the lack of sensitivity of the rapid centrifugation method used to measure the cellular accumulation of phenanthrene and anthracene, whereas the growth-based assays used to assess antibiotic and toluene efflux are more sensitive to small

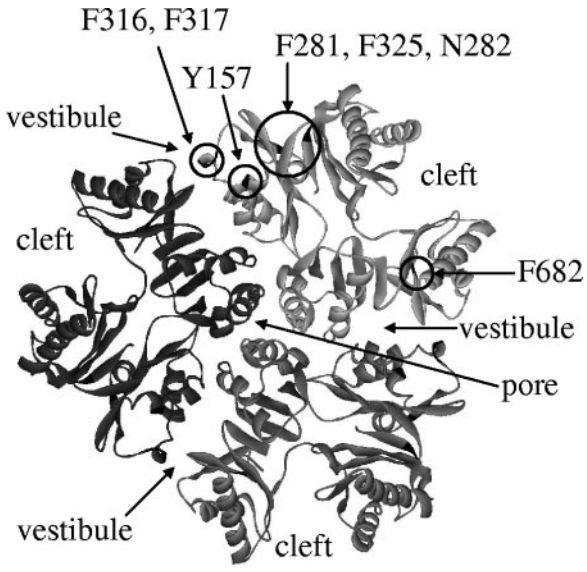

FIG. 4. Predicted structure of the periplasmic pore domain of EmhB. The pore domain is viewed from the top of the protein perpendicular to the plane of the membrane, showing the positions of the central pore, vestibules, and clefts. The locations of the residues targeted for mutagenesis are indicated.

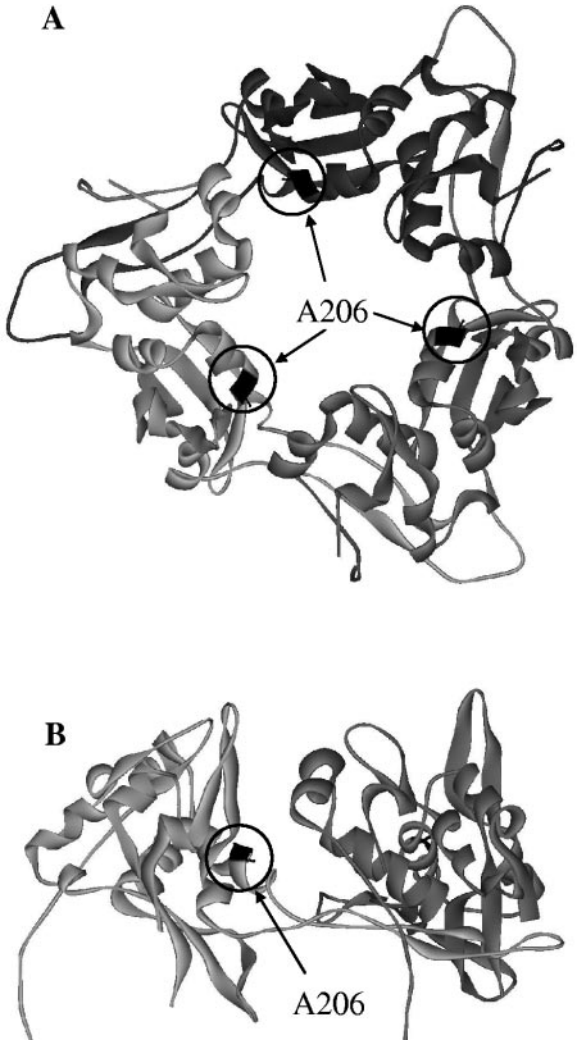

FIG. 5. Predicted model of the outer membrane protein docking domain of EmhB. The domain is viewed from the top of the protein perpendicular to the plane of the membrane (A) and from the side of the protein with the rear monomer removed (B). The location of the A206 residue is indicated.

changes in the cellular accumulation of these substrates. The A206S mutation responsible for the enhanced efflux activity mapped to the outer membrane protein docking domain of the efflux pump (Fig. 5), and this residue is highly conserved among the ArpB, SrpB, TtgB, TtgE, TtgH, MexB, and AcrB multidrug and toluene efflux pumps (Table 1).

DISCUSSION

In this study, the activity of the RND efflux pump EmhB, as well as site-specific mutations of the EmhB pump, from *P. fluorescens* cLP6a was explored to gain insight into the function of this family of transport proteins. The EmhB efflux pump has a broader substrate specificity than previously proposed (4, 9). In addition to polycyclic aromatic hydrocarbons, EmhB pumps toluene and a wide range of hydrophobic antibiotics, including chloramphenicol, nalidixic acid, rhodamine 6G, dequalinium, and ciprofloxacin. This broad substrate specificity makes EmhB advantageous for studying the effects of mutations on efflux activity. Addition of the histidine tag on EmhB did not affect transport activity for polycyclic aromatic hydrocarbons but did decrease the efficiency of the efflux pump for antibiotics and toluene (Table 1), likely due to the nonlinear response of growth-based assays. Nonlinear responses in growth-based assays were observed by Li et al. (14), who measured a 16-fold reduction in tetracycline resistance, but only a threefold increase in tetracycline accumulation, for a MexAB-OprM-deficient *P. aeruginosa* strain compared to levels for the wild type. Despite differences in the activity of the histidine-tagged $EmhB_{His}$ relative to that of the wild-type pump, *P. fluorescens* cLP6a-1 expressing $EmhB_{His}$ showed efflux activity for polycyclic aromatic hydrocarbons, hydrophobic antibiotics, and toluene compared to the efflux pump-deficient strain (Table 1). Thus, mutations were introduced in $EmhB_{His}$ to confirm expression of the mutant pumps (Fig. 2) and to compare the activity of the mutant pumps for polycyclic aromatic hydrocarbons, antibiotics, and toluene relative to that of $EmhB_{His}$ (Table 1).

Recently, Yu et al. (31) crystallized the *E. coli* AcrB efflux pump with bound substrates and identified amino acids within the central cavity that interacted with various drugs. Of the central cavity residues investigated in this study, A385 and F386 had been shown to interact with rhodamine 6G; F386, D99, and D101 were involved in dequalinium binding; and A385, F458, and F459 were implicated in ciprofloxacin binding in the AcrB crystal structure (31). The involvement of the A385 residue in efflux activity for rhodamine 6G was confirmed by the A384P/A385Y mutation in $EmhB_{His}$ (Table 1). Introduction of the bulkier proline and tyrosine side chains may have caused localized disruption of the central cavity structure, making rhodamine 6G binding unfavorable. The F386A mutation in $EmhB_{His}$ did not affect resistance to rhodamine 6G but did significantly decrease resistance to dequalinium fourfold (Table 1). Recently, Yu et al. (32) reported similar results for an AcrB F386A mutant. Furthermore, the N99A and D101A mutations in $EmhB_{His}$ significantly reduced pump activity for dequalinium, as expected from the crystal structure data (31). Ciprofloxacin interacted with the A385, F458, and F459 residues in the AcrB crystal structure (31); however, the ciprofloxacin MICs for the A384P/A385Y, F458A, and F459A mutations in $EmhB_{His}$ showed only twofold decreases compared to that of the control $EmhB_{His}$ (Table 1). The failure to observe a significant effect on ciprofloxacin resistance with the F458A and F459A mutations suggests that mutation of only one of the phenylalanines was not sufficient to disrupt the binding of ciprofloxacin. Crystallization studies with the *Staphylococcus aureus* QacR multidrug repressor protein demonstrated the flexibility of a hydrophobic cavity to accommodate multiple substrates by shifting the drug-binding site (27). The hydrophobic nature and the flexibility of multidrug-binding sites within the central cavity of RND efflux pumps likely explain the failure to observe significant effects on ciprofloxacin resistance, as well as on chloramphenicol and nalidixic acid resistance and aromatic hydrocarbon transport, with the mutations to the lower region of the EmhB central cavity.

For the majority of EmhB substrates, transport activity was dependent upon the presence of a carboxyl group at position 101 located at the top of the central cavity (Table 1). Cysteine-

scanning mutagenesis studies with the AcrB pump in *E. coli* also demonstrated the importance of D101 in antibiotic resistance for chloramphenicol and nalidixic acid as well as for tetracycline, acriflavin, and erythromycin (18). An *E. coli* strain expressing a D101A mutation in AcrB showed increased susceptibility to some (acriflavin, tetracycline, dequalinium, erythromycin, and novobiocin), but not all, antibiotics tested, prompting Yu et al. (32) to propose that D101 may be involved in ligand binding. However, the D101A mutation in $EmhB_{His}$ affected the transport of uncharged polycyclic aromatic hydrocarbons, suggesting that the carboxyl group may play an important role in stabilizing protein-protein interactions between the pump subunits in addition to binding charged ligands, such as dequalinium.

RND efflux pumps have a large periplasmic domain, which is distinct from those of other families of multidrug transporters and is believed to be responsible for substrate selectivity and capture (2, 6, 15, 29). In addition to substrate recognition, the periplasmic domain is involved in protein-protein interactions between the RND efflux pump subunits, as well as with the membrane fusion protein and outer membrane factor protein. Although the structures of the mutant EmhB pumps were not determined, the mutations generated in the periplasmic domain likely affected the overall structure of the pump, due to the broad effects on activity that were observed. The two mutations near the vestibules (F316 and F317) showed moderate loss of efflux activity for a number of substrates (Table 1). Middlemiss and Poole (16) also attributed the loss of efflux activity for two mutations in the MexB vestibule region, S462F and E864K, to alterations in the structure of the pump. Thus, the vestibule region likely plays an important role in stabilizing the pump structure. Similarly, the phenylalanines at positions 281 and 325 in EmhB are essential either by stabilizing the three-dimensional conformation of the pump or by interacting with the membrane fusion protein or outer membrane protein.

Surprisingly, the activity of $EmhB_{His}$ for antibiotics and toluene was enhanced by the A206S mutation, which mapped to the interface of the outer membrane protein docking domain (Fig. 5). The outer membrane protein docking domain of RND efflux pumps has been proposed to act as a funnel, which interacts with the outer membrane protein and opens to allow substrates entry into the outer membrane channel (19). The A206S mutation may maintain the funnel in a more open state or may enhance interaction between the RND pump and the outer membrane protein, thereby creating a more efficient efflux complex. Middlemiss and Poole (16) also identified a mutation (G220S) in the outer membrane protein docking domain of the MexB pump from *P. aeruginosa* that reduced efflux activity for all antibiotics tested. The G220 residue is located on the protruding arm of the efflux pump subunit, which inserts into a pocket in the neighboring subunit. The protruding arm of the efflux pump may be involved in opening and closing the funnel, and the G220S mutation may lock the efflux pump in a closed state. Middlemiss and Poole (16) isolated a V203M/G581D double mutation that restored antibiotic resistance of the G220S mutant pump to wild-type levels. Like A206 in EmhB, the V203M mutation in MexB may maintain the pump in an open state, compensating for the G220S mutation.

The results for the A206S mutation in EmhB presented here, as well as for the G220S mutation in MexB reported by Middlemiss and Poole (16), provide evidence for the role of the outer membrane protein docking domain in the function of RND efflux pumps. Further examination of this region will provide valuable information regarding the mechanism by which the efflux pump opens to allow substrates to enter the outer membrane protein. Since this mechanism is likely a universal feature of RND efflux pumps, the outer membrane protein docking domain provides an excellent target for pump inhibitors. An inhibitor that locks the funnel in a closed state could successfully eliminate efflux pump-mediated antibiotic resistance.

ACKNOWLEDGMENTS

We thank B. Borlé for her assistance in the construction and analysis of the site-directed mutants.

This work was supported by NSERC Discovery grants to M.R.G. and J.M.F. E.M.H. gratefully acknowledges funding from the Izaak Walton Killam Memorial Scholarship, NSERC, and the Province of Alberta Graduate Fellowship program.

REFERENCES

1. **Aires, J. R., T. Köhler, H. Nikaido, and P. Plesiat.** 1999. Involvement of an active efflux system in the natural resistance of *Pseudomonas aeruginosa* to aminoglycosides. Antimicrob. Agents Chemother. **43:**2624–2628.
2. **Aires, J. R., and H. Nikaido.** 2005. Aminoglycosides are captured from both periplasm and cytoplasm by the AcrD multidrug efflux transporter of *Escherichia coli*. J. Bacteriol. **187:**1923–1929.
3. **Aires, J. R., J.-C. Pechère, C. van Delden, and T. Köhler.** 2002. Amino acid residues essential for function of the MexF efflux pump protein of *Pseudomonas aeruginosa*. Antimicrob. Agents Chemother. **46:**2169–2173.
4. **Bugg, T., J. M. Foght, M. A. Pickard, and M. R. Gray.** 2000. Uptake and active efflux of polycyclic aromatic hydrocarbons by *Pseudomonas fluorescens* LP6a. Appl. Environ. Microbiol. **66:**5387–5392.
5. **Eda, S., H. Maseda, and T. Nakae.** 2003. An elegant means of self-protection in Gram-negative bacteria by recognizing and extruding xenobiotics from the periplasmic space. J. Biol. Chem. **278:**2085–2088.
6. **Elkins, C. A., and H. Nikaido.** 2002. Substrate specificity of the RND-type multidrug efflux pumps AcrB and AcrD of *Escherichia coli* is determined predominantly by two large periplasmic loops. J. Bacteriol. **184:**6490–6498.
7. **Guan, L., and T. Nakae.** 2001. Identification of essential charged residues in transmembrane segments of the multidrug transporter MexB of *Pseudomonas aeruginosa*. J. Bacteriol. **183:**1734–1739.
8. **Guex, N., and M. C. Peitsch.** 1997. SWISS-MODEL and the Swiss-PdbViewer: an environment for comparative protein modeling. Electrophoresis **18:**2714–2723.
9. **Hearn, E. M., J. J. Dennis, M. R. Gray, and J. M. Foght.** 2003. Identification and characterization of the *emhABC* efflux system for polycyclic aromatic hydrocarbons in *Pseudomonas fluorescens* cLP6a. J. Bacteriol. **185:**6233–6240.
10. **Horton, R. M., H. D. Hunt, S. N. Ho, J. K. Pullen, and L. R. Pease.** 1989. Engineering hybrid genes without the use of restriction enzymes: gene splicing by overlap extension. Gene **77:**61–68.
11. **Jorgensen, J. H., J. D. Turnridge, and J. A. Washington.** 1999. Antibacterial susceptibility tests: dilution and disk diffusion methods, p. 1526–1543. *In* P. R. Murray, E. J. Baron, M. A. Pfaller, F. C. Tenover, and R. H. Yolken (ed.), Manual of clinical microbiology, 7th ed. American Society for Microbiology, Washington, D.C.
12. **Kieboom, J., and J. A. M. de Bont.** 2001. Identification and molecular characterization of an efflux system involved in *Pseudomonas putida* S12 multidrug resistance. Microbiology **147:**43–51.
13. **Kieboom, J., J. J. Dennis, J. A. M. de Bont, and G. J. Zylstra.** 1998. Identification and molecular characterization of an efflux pump involved in *Pseudomonas putida* S12 solvent tolerance. J. Biol. Chem. **273:**85–91.
14. **Li, X. Z., H. Nikaido, and K. Poole.** 1995. Role of MexA-MexB-OprM in antibiotic efflux in *Pseudomonas aeruginosa*. Antimicrob. Agents Chemother. **39:**1948–1953.
15. **Mao, Q., M. S. Warren, D. S. Black, T. Satou, T. Murata, T. Nishino, N. Gotoh, and O. Lomovskaya.** 2002. On the mechanism of substrate specificity by resistance nodulation division (RND)-type multidrug resistance pumps: the large periplasmic loops of MexD from *Pseudomonas aeruginosa* are involved in substrate recognition. Mol. Microbiol. **46:**889–901.

16. **Middlemiss, J. K., and K. Poole.** 2004. Differential impact of MexB mutations on substrate selectivity of the MexAB-OprM multidrug efflux pump of *Pseudomonas aeruginosa*. J. Bacteriol. **186:**1258–1269.
17. **Mosqueda, G., and J.-L. Ramos.** 2000. A set of genes encoding a second toluene efflux system in *Pseudomonas putida* DOT-T1E is linked to the *tod* genes for toluene metabolism. J. Bacteriol. **182:**937–943.
18. **Murakami, S., N. Tamura, A. Saito, T. Hirata, and A. Yamaguchi.** 2004. Extramembrane central pore of multidrug exporter AcrB in *Escherichia coli* plays an important role in drug transport. J. Biol. Chem. **279:**3743–3748.
19. **Murakami, S., R. Nakashima, E. Yamashita, and A. Yamaguchi.** 2002. Crystal structure of bacterial multidrug efflux transporter AcrB. Nature **419:**587–593.
20. **Nikaido, H.** 1996. Multidrug efflux pumps of gram-negative bacteria. J. Bacteriol. **178:**5853–5859.
21. **Poole, K.** 2004. Efflux-mediated multiresistance in Gram-negative bacteria. Clin. Microbiol. Infect. **10:**12–26.
22. **Poole, K., N. Gotoh, H. Tsujimoto, Q. Zhao, A. Wada, T. Yamasaki, S. Neshat, J. Yamagishi, X. Z. Li, and T. Nishino.** 1996. Overexpression of the *mexC-mexD-oprJ* efflux operon in *nfxB*-type multidrug-resistant strains of *Pseudomonas aeruginosa*. Mol. Microbiol. **21:**713–724.
23. **Ramos, J. L., E. Duque, M. T. Gallegos, P. Godoy, M. I. Ramos-Gonzalez, A. Rojas, W. Terán, and A. Segura.** 2002. Mechanisms of solvent tolerance in Gram-negative bacteria. Annu. Rev. Microbiol. **56:**743–768.
24. **Ramos, J. L., E. Duque, P. Godoy, and A. Segura.** 1998. Efflux pumps involved in toluene tolerance in *Pseudomonas putida* DOT-T1E. J. Bacteriol. **180:**3323–3329.
25. **Rojas, A., E. Duque, G. Mosqueda, G. Golden, A. Hurtado, J. L. Ramos, and A. Segura.** 2001. Three efflux pumps are required to provide efficient tolerance to toluene in *Pseudomonas putida* DOT-T1E. J. Bacteriol. **183:**3967–3973.
26. **Sambrook, J., E. F. Fritsch, and T. Maniatis.** 1989. Molecular cloning: a laboratory manual, 2nd ed. Cold Spring Harbor Laboratory Press, Cold Spring Harbor, N.Y.
27. **Schumacher, M. A., M. C. Miller, and R. G. Brennan.** 2004. Structural mechanism of the simultaneous binding of two drugs to a multidrug-binding protein. EMBO J. **23:**2923–2930.
28. **Thompson, J. D., T. J. Gibson, F. Plewniak, F. Jeanmougin, and D. G. Higgins.** 1997. The ClustalX windows interface: flexible strategies for multiple sequence alignment aided by quality analysis tools. Nucleic Acids Res. **25:**4876–4882.
29. **Tikhonova, E. B., Q. Wang, and H. I. Zgurskaya.** 2002. Chimeric analysis of the multicomponent multidrug efflux transporters from gram-negative bacteria. J. Bacteriol. **184:**6499–6507.
30. **West, S. E. H., H. P. Schweizer, C. Dall, A. K. Sample, and L. J. Runyen-Janecky.** 1994. Construction of improved *Escherichia-Pseudomonas* shuttle vectors derived from pUC18/19 and sequence of the region required for their replication in *Pseudomonas aeruginosa*. Gene **148:**81–86.
31. **Yu, E. W., G. McDermott, H. I. Zgurskaya, H. Nikaido, and D. E. Koshland, Jr.** 2003. Structural basis of multiple drug-binding capacity of the AcrB multidrug efflux pump. Science **300:**976–980.
32. **Yu, E. W., J. R. Aires, G. McDermott, and H. Nikaido.** 2005. A periplasmic drug-binding site of the AcrB multidrug efflux pump: a crystallographic and site-directed mutagenesis study. J. Bacteriol. **187:**6804–6815.